

Raman study of SiC fibres made from polycarbosilane

Y. SASAKI, Y. NISHINA

The Research Institute for Iron, Steel and Other Metals, Tohoku University, Sendai 980, Japan

M. SATO, K. OKAMURA

The Oarai Branch, The Research Institute for Iron, Steel and Other Metals, Tohoku University, Oarai, Ibaraki-Ken 311-13, Japan

We have examined the evolution of Raman spectra of SiC fibres through structural and compositional transformations caused by heat treatment. The SiC fibre was made from polycarbosilane. Raman spectra of the SiC fibre indicate that it consists of (i) amorphous or microcrystalline SiC, (ii) carbon microcrystals, and (iii) silicon oxide. The amount of microcrystalline carbon in the fibre increases with heat treatment temperature up to 1400°C, and it decreases abruptly in those fibres heat treated above 1500°C. The tensile strength of the fibre drops virtually to zero after the heat treatment at 1500°C. Carbon microcrystals are precipitated from the Si-C random network with excess carbon, and they are distributed uniformly in the fibre. These carbon particles suppress the growth of SiC crystals. It is shown that the carbon microcrystals play an important role in maintaining the high mechanical strength of the SiC fibre.

1. Introduction

During the last two decades, various kinds of ceramic fibre have been developed such as those made from carbon, SiC, alumina etc. [1]. These fibres have common advantages for application to structural components, i.e. lightness in weight, high tensile strength and high modulus. They usually consist of small amorphous or crystalline particles. The mechanical strength of these kinds of fibres is determined mainly by the bonds between the particles rather than the constituent particles themselves.

The fabrication process of SiC fibres from an organic precursor has been developed by Yajima and co-workers [2]. The organic fibre made from polycarbosilane is converted to inorganic fibre through pyrolytic heat treatment to about 800°C. The molecular structure of the polycarbosilane and the pyrolysis process have been studied by nuclear magnetic resonance (NMR) and optical absorption measurements [3]. Furthermore, X-ray diffraction studies have revealed the growth of SiC microcrystals in the heat treatment of the inorganic fibre [2]. The physical properties of the fibres can be controlled by the final heat treatment temperature (HTT). Increase in the particle (or crystal) size can be a cause of variations in the mechanical and/or thermal properties of the fibre. The tensile strength of SiC fibre reaches a maximum value (up to 3.5 GPa) for HTT = 1200°C, and it decreases for higher HTT [4]. This tensile strength is comparable to that of carbon fibres, and furthermore, these SiC fibres can maintain such a strength even in oxidizing environment up to $\approx 1200^\circ\text{C}$ [2].

The existence of oxygen in the fibre has been confir-

med by chemical analyses [4]. X-ray diffraction spectra indicate that the oxygen atoms form silicon oxides [3]. As a result of reaction between oxygen and carbon, CO gas evolution is observed at $\sim 1300^\circ\text{C}$ and $\sim 1500^\circ\text{C}$ in the fibres cured in air. A decrease in the tensile strength shows a correlation with the CO gas evolution [5]. Thus, oxygen in the fibre seems to be correlated strongly with the mechanical properties of the fibre at high temperatures. Chemical analyses of the fibre indicate the existence of excess carbon with respect to the stoichiometrical value for SiC [4]. The role of the excess carbon has not so far been studied.

Since the vibrational spectrum is sensitive to the nature of the chemical bonding between nearest neighbours, Raman spectroscopy is useful for the study of the short-range structure of solids. Also the Raman spectrum reflects the vibrational mode in a long-range order of 1 to 100 nm. For semiconductor microcrystals ($\lesssim 10$ nm) such as germanium, silicon or GaP the Raman spectra are similar to those in amorphous states, while they are crystal-like for crystals larger than 10 nm [6-8]. The disorder induced by ion implantation has been known to change the Raman spectra. As the dose (or disorder) increases, the Raman spectra become broadened, and for an extremely high dose (or highly damaged crystal), they become amorphous-like [9]. Thus Raman spectroscopy is useful for the study of a wide range ($\lesssim 100$ nm) of structure of solids.

The purpose of this paper is to determine the correlation between the mechanical properties and the microscopic structure of SiC fibre with respect to HTT. We have analysed the Raman spectra of the fibres in order to deduce their microscopic structure.

Furthermore, X-ray diffraction profiles and transmission electron microscope (TEM) photographs have been obtained to estimate the size of SiC particles in the fibre. We discuss the relationship between the microscopic structure and tensile strength. Preliminary results have been published elsewhere [10].

2. Experimental procedure

The SiC fibres used in this work have been derived from a polycarbosilane precursor through curing in air at 190°C for one hour, then through heat treatment at temperatures between 700 and 1900°C in argon gas atmosphere for another hour. The detailed fabrication process has been described in the literature [2].

Raman spectra were obtained with a double-grating monochromator and a photon counting system. The light source was an Ar⁺ laser beam (488 nm, 20 mW) focused to 0.1 × 2.5 mm² by a cylindrical lens. A bundle of SiC fibres was placed in air for the Raman measurement. Joule heating caused by the laser irradiation turned out to be negligible in the experimental conditions where the laser power was changed from 10 to 40 mW. The measured Raman spectra were not corrected for the spectral responses of the monochromator and photomultiplier. The correction may enhance the intensity at larger Stokes shifts. Such a correction, however, does not affect the semi-quantitative argument given in this paper.

X-ray diffraction patterns were obtained with a diffractometer using CuK α radiation with a pyrolytic-graphite monochromator as the characteristic X-rays. The fibres were pulverized in an agate mortar. The TEM photographs were taken with a 200 keV high-resolution electron microscope.

3. Experimental results

3.1. Raman spectra

Fig. 1 shows the Raman spectra of SiC fibres heat treated at various temperatures. A strong photoluminescence background from the fibre with HTT = 700°C grossly masks the Raman signal so that the latter cannot be discriminated. The Raman spectra of the fibres heat treated below 1400°C are quite different from those treated above 1500°C. The Raman spectra for lower HTT fibres consist of broad lines at around 400, 750, 1350 and 1600 cm⁻¹. On the other hand, a sharp line shows up at 795 cm⁻¹ in the spectra of the higher HTT fibres, and the features at around 1350 and 1600 cm⁻¹ becomes suppressed. We have deconvoluted the Raman spectra into several lines by a curve fit. Fig. 2 shows an example for lower HTT fibres and Fig. 3 for higher HTT fibres, respectively. In both cases, we assume a Lorentzian tail due to stray light in the monochromator and a constant background as shown by dashed lines. The background may be due to photoluminescence from the fibre.

The density of states (DOS) of phonons in 3C-SiC shows peaks due to the zone-edge transverse acoustic (TA) phonon at ~300 cm⁻¹ and the zone-edge transverse optical (TO) phonon at ~750 cm⁻¹ according to theoretical calculations [11]. These peaks are located close to the two broad Raman lines at ~400 and

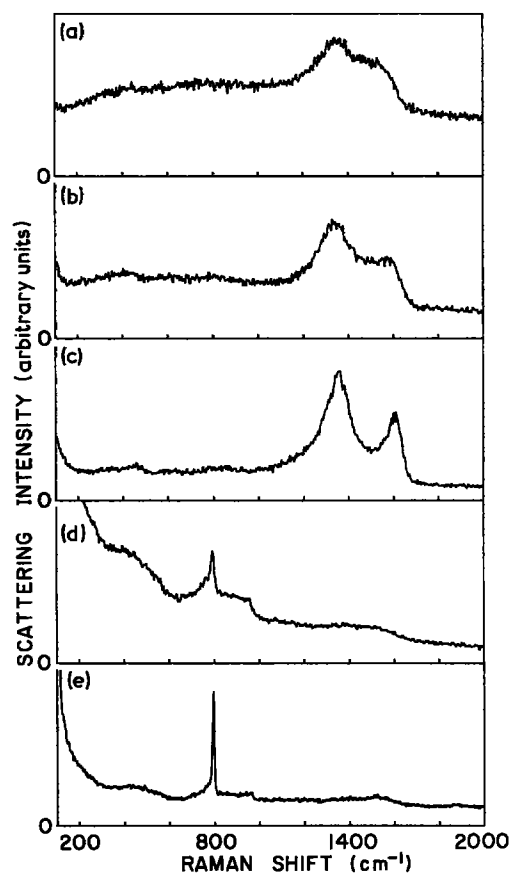


Figure 1 Raman spectra of SiC fibres heat-treated at various temperatures (HTT): (a) 1000, (b) 1200, (c) 1400, (d) 1500, (e) 1700°C.

~800 cm⁻¹. It is well accepted that the Raman spectra of amorphous solids reflect the phonon DOS of the corresponding crystal [12]. It is reasonable, therefore, to assign the origin of the Raman lines at ~400 and ~800 cm⁻¹ to amorphous SiC. The line-widths of these two Raman lines are 400 to 600 cm⁻¹ for fibres of HTT ≤ 1400°C, and they decrease down to about 200 cm⁻¹ for fibres of HTT ≥ 1500°C. The line-narrowing suggests that the fluctuation in the bond angle decreases [13]. Since no crystalline-origin peak is observed in the fibres heat-treated below 1400°C, SiC in these fibres is either amorphous or microcrystalline with the size smaller than ~10 nm.

In 3C-SiC, which is the most frequently observed polytype below 2000°C [14], the energy of the zone-centre TO phonon (TO(Γ)) has been reported to be 796 cm⁻¹ and that of the zone-centre longitudinal optical (LO(Γ)) phonon to be 973 cm⁻¹ [15, 16]. The sharp line at 795 cm⁻¹ is attributed to the TO(Γ) phonon. The intensity of the LO(Γ) line is comparable to that of the TO(Γ) line in crystalline SiC, whereas the LO(Γ) line is very weak and shifted toward lower frequency by about 10 cm⁻¹ in the fibres heat-treated between 1500 and 1700°C. The Raman shift (766 cm⁻¹) of the weak shoulder at the lower frequency side of TO(Γ) is equal to the frequency of the zone-centre phonon folded from the zone-edge (L point) in 4H or 6H-SiC [15, 17]. The 3C and 2H polytypes are stable in the temperature range from ~1300°C to ~1600°C, but the 2H polytype is transformed to 3C polytype at a temperature between 1400 and 1800°C [14, 18]. The above arguments on the frequency of the

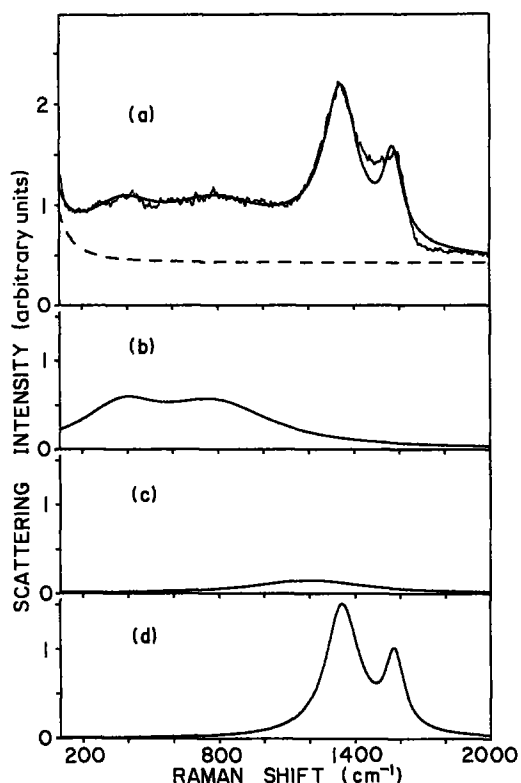


Figure 2 (a) Curve fit to the Raman spectrum of the fibre with $\text{HTT} = 1200^\circ\text{C}$. The thin solid line shows the experimental spectrum and the bold line is the sum of the components (b) to (d). The dashed line represents the Rayleigh tail on a flat background. (b) to (d) show the results of deconvolution for the curve fit: (b) amorphous SiC, (c) Si-O, (d) carbon.

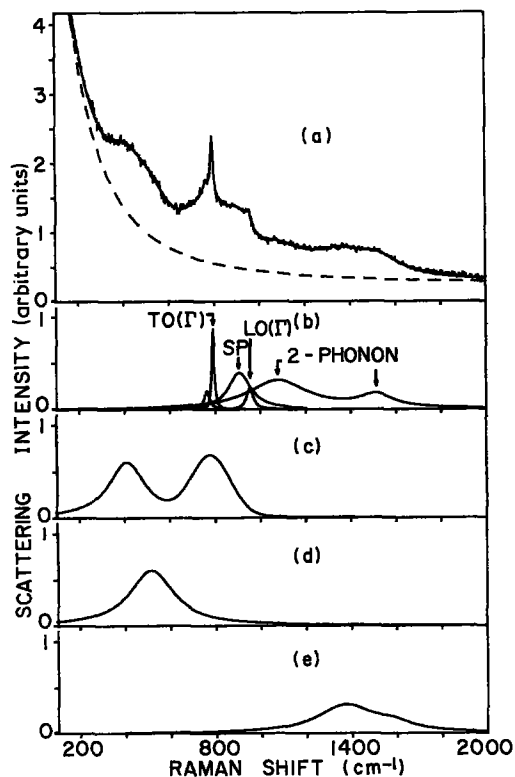


Figure 3 (a) Curve fit to the Raman spectrum of the fibre with $\text{HTT} = 1500^\circ\text{C}$. The thin solid line shows the experimental spectrum and the bold line is the sum of the components (b) to (e). The dashed line represents the Rayleigh tail and a flat background. The results of the deconvolution by the curve fit are shown in (b) to (e): (b) crystalline SiC, (c) amorphous SiC, (d) Si-O, (e) carbon. Notations for the peaks in (b) are explained in the text.

766 cm^{-1} line as well as on the polytype stability lead to the assignment for the structure; i.e. it comes from the zone-folded optical phonon of 2H-SiC, which is not the polytype predominating in the fibre.

In particles smaller than about 100 nm, the surface-phonon polariton (SPP), especially the so-called Fröhlich mode, plays an important role in the Raman spectra [19]. Following the effective medium theory [20], the expected frequency for such a surface polariton mode is 934 cm^{-1} assuming the dielectric constant of the medium (ϵ_m) surrounding the SiC particle to be unity, or 910 cm^{-1} for $\epsilon_m = 2$. Here we use a value for the static dielectric constant of 10.0 [11]. On the other hand, the result of the curve fit to the experimental spectra requires a line noted as SPP at 910 to 920 cm^{-1} . Since the peak position is consistent with the calculated surface polariton frequency for $\epsilon_m = 2$, we assign the SP line in Fig. 3c to the SPP. The existence of silicon oxide and carbon in the fibre, as explained later, gives a value of ϵ_m higher than that of air or vacuum. The peak at 1525 cm^{-1} corresponds to the two-phonon line observed in SiC single crystals [15]. The existence of the Raman lines due to $\text{TO}(\Gamma)$, the zone-folded optical phonon and the SPP indicate that SiC in the fibres heat-treated above 1500°C is microcrystalline with a size of 10 to 100 nm.

Two dominant Raman peaks are observed at 1350 and 1600 cm^{-1} in graphitic carbon microcrystals. The intensity ratio of the two lines is a good measure of the crystallite size in the a -plane [21]. In the SiC fibre heat-treated below 1400°C , we find two peaks at frequencies similar to those observed in carbon. Thus the doublet at ~ 1350 and $\sim 1600\text{ cm}^{-1}$ is attributed to carbon microcrystals. The average crystal size in the the a -plane is estimated to be less than 5 nm from the relative intensity of the two Raman lines [21]. A rather large discrepancy in the curve-fitting for the 1600 cm^{-1} line is attributed to Fano interference between the 1600 cm^{-1} line and the two-phonon continuous background [22]. In the fibres heat-treated above 1500°C , these carbon lines diminish and their line-widths increase by a factor of two compared to those with $\text{HTT} = 1400^\circ\text{C}$. The presence of the carbon lines indicates that excess carbon atoms segregate to form carbon microcrystals. In X-ray diffraction profiles, carbon-related lines are not observed at all because of the small atomic scattering factor compared with silicon.

Although the measured Raman spectra do not clearly show any other line besides those explained above, additional weak Raman lines have to be present for a good curve fit as shown in Figs 2 and 3. These additional lines are located at $\sim 1200\text{ cm}^{-1}$ for the fibres of $\text{HTT} \leq 1400^\circ\text{C}$ (Fig. 2) and at ~ 500 and $\sim 1100\text{ cm}^{-1}$ for those of $\text{HTT} \geq 1500^\circ\text{C}$ (Fig. 3). These frequencies are close to the bond bending ($\sim 500\text{ cm}^{-1}$) and stretching ($\sim 1100\text{ cm}^{-1}$) vibrations in SiO_2 glass [23]. The 1100 cm^{-1} Raman line is very weak in pure SiO_2 glass but it becomes stronger in the glasses with non-bridging (or partially ionized) oxygen atoms [24]. Since the existence of amorphous SiO_2 has been confirmed in our fibres by X-ray analyses, these Raman lines may be assigned as

bending or stretching vibrations of the Si-O bond. For the fibres of $\text{HTT} \leq 1400^\circ\text{C}$, therefore, one may attribute the 1200 cm^{-1} line to Si-O stretching vibrations. For the same reason, the 500 cm^{-1} line in the fibres of $\text{HTT} \geq 1500^\circ\text{C}$ corresponds to bending vibrations of the Si-O bond.

A 1100 cm^{-1} line, however, exists also in crystalline SiC and it has been assigned as a two-phonon line [15]. The ratio of the intensities of the 1100 cm^{-1} line to 1520 cm^{-1} line in SiC crystal is comparable to the corresponding ratio in our fibres with a sharp TO-phonon line ($\text{HTT} \geq 1500^\circ\text{C}$). Thus we attribute the 1100 cm^{-1} line in the fibres with $\text{HTT} \geq 1500^\circ\text{C}$ as a two-phonon line of crystalline SiC. Since we have not observed X-ray diffraction lines due to the oxide in our fibres with $\text{HTT} \geq 1500^\circ\text{C}$, the particle size of the oxide, if it exists at all, has to be extremely small; i.e. oxygen may be contained as an impurity or terminating dangling bonds at the surface of microcrystals.

3.2. Dependences of fibre compositions on HTT

The integrated Raman intensities are estimated from the width and the amplitude of deconvoluted lines. Fig. 4 shows the HTT dependence of the relative integrated intensities for SiC, carbon and silicon oxide components in the Raman spectra. The intensity for SiC includes the lines due to amorphous and crystalline states. The SiC component is nearly constant up to 1200°C beyond which it decreases, and then it increases abruptly at 1500°C . The carbon component increases with HTT up to 1400°C , then it suddenly decreases at 1500°C . The carbon component increases with HTT up to 1400°C , then it suddenly decreases at 1500°C . These complementary variations of the two components in their Raman intensities suggest the following model: excess carbon in carbon-rich amorphous SiC precipitates to form carbon particles up to $\text{HTT} = 1400^\circ\text{C}$, and then it disappears above 1500°C . CO gas evolution due to the reaction between the carbon and oxygen in the fibres is observed at around 1300 and 1500°C [5]. These gas evolution

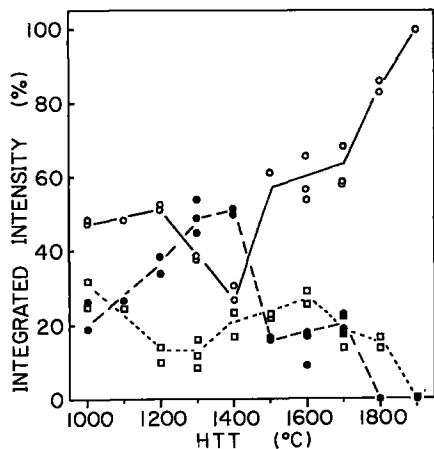


Figure 4 Integrated Raman intensities for the components of (○) SiC, (●) carbon and (□) Si-O vibrations. The SiC component is a summation of the Raman lines due to amorphous and crystalline states.

processes may compete with the precipitation of the carbon. The carbon component in the Raman spectra virtually vanishes for $\text{HTT} \geq 1800^\circ\text{C}$, whereas the Si-O line remains up to $\text{HTT} \sim 1900^\circ\text{C}$. Thus the amount of excess carbon is expected to be less than or comparable to that of the oxygen contained in the fibre.

We need to know the Raman scattering efficiency in order to deduce the quantitative amount of constituents from Raman spectra. The ratio of the efficiency of graphite to that of SiC or SiO_2 has not been reported. It is, however, possible to estimate the ratio by analogy with the Raman efficiency for graphite, silicon [25] and diamond [26] measured for the incident laser wavelength of 514.5 nm . Assuming that the magnitude of the Raman tensor component in SiC is given by an average between the values for silicon and diamond, we find that the Raman efficiency for SiC is 1/10 of that of graphite. This difference in the Raman efficiencies has been suggested for carbon-rich SiC film prepared by sputtering [27, 28]. Thus the amount of carbon particles is roughly estimated to be about 20 vol % with respect to SiC in the fibres with, for example, $\text{HTT} = 1400^\circ\text{C}$.

3.3. X-ray diffraction and TEM observations

Fig. 5 shows the apparent crystal size of 3C-SiC as estimated from the (1 1 1) diffraction line width. The average SiC particle size is deduced from the TEM photographs and is given in Fig. 5. Also plotted in the figure is the tensile strength of the fibre against HTT. The crystal/particle size of SiC jumps between $\text{HTT} = 1400^\circ\text{C}$ and 1500°C , whereas the tensile strength drops virtually to zero in the same HTT range. The jump in the crystal/particle size occurs at the same temperature as the second CO gas evolution. The particle size of SiC as estimated from TEM photographs is comparable to that of SiC crystals

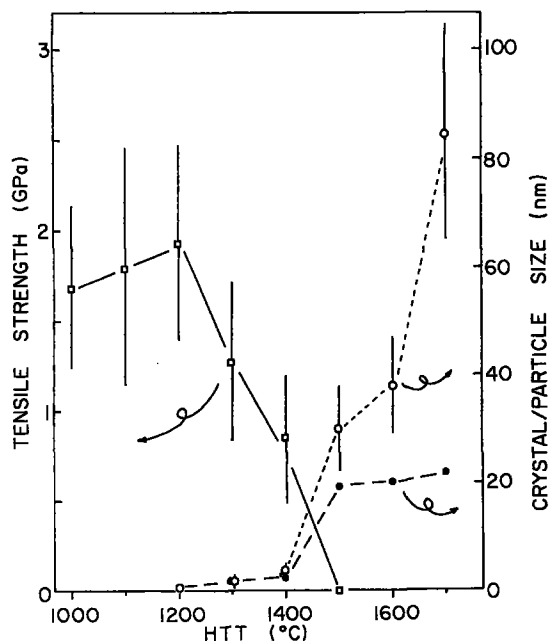


Figure 5 (●) Crystal size and (○) particle size of SiC plotted as a function of HTT; (□) shows tensile strength of the SiC fibre. CO gas evolution is observed at around 1300 and 1500°C . The crystal size grows up to 160 nm for $\text{HTT} = 1800^\circ\text{C}$.

deduced from X-ray diffraction spectra for $\text{HTT} \leq 1400^\circ\text{C}$, whereas the particle size is much larger than the crystal size if $\text{HTT} \geq 1500^\circ\text{C}$. Coalescence of the SiC crystals, therefore, takes place above 1500°C .

Lattice fringes in the TEM image show up in the fibres with $\text{HTT} \geq 1200^\circ\text{C}$. This observation indicates that the nucleation starts at $\sim 1200^\circ\text{C}$. The sizes of the crystallized particles are larger for higher HTT. The fibre with the highest tensile strength is produced for $\text{HTT} = 1200^\circ\text{C}$, where the nucleation of SiC starts. The SiC in this fibre, therefore, is mostly amorphous, as suggested from the analysis of the Raman spectra in Section 3.1. The amorphous-like Raman spectra turn into the crystal-like between $\text{HTT} = 1400$ and 1500°C as explained in Section 3.1. In the same temperature range, the average crystal size of SiC grows from ~ 3 to ~ 20 nm. The Raman spectra may be transformed from amorphous-like to crystal-like at a critical crystal size of about 10 nm. This size is comparable to that reported for germanium, silicon and GaP [6–8].

4. Discussion

Since SiC fibres in the present investigation are fabricated from precursor materials containing excess carbon, they probably consist of carbon-rich Si–C random networks after organic to inorganic transformation at $\sim 800^\circ\text{C}$ [3]. The Raman spectrum for the $\text{HTT} = 800^\circ\text{C}$ fibre shows the carbon doublet at ~ 1350 and $\sim 1600\text{cm}^{-1}$. The C_6 -ring structure, therefore, starts to develop right after, or in the course of, the organic–inorganic transformation. The number and/or size of carbon clusters keeps growing up to $\text{HTT} = 1400^\circ\text{C}$ as explained in Section 3.2. Simultaneously, the size of the SiC crystal increases as mentioned in Section 3.3. The growth of the crystal by heat treatment at higher temperatures reduces its tensile strength through the increase in the density of grain boundaries, because bonds between the grains are much weaker than those between atoms in crystalline or amorphous states. In the fibre with the highest tensile strength ($\text{HTT} = 1200^\circ\text{C}$), a small number of carbon and SiC microcrystals (~ 1 nm) are distributed uniformly in carbon-rich amorphous SiC.

SiC fibres produced without a curing process contain a very low density of oxygen compared with the fibres cured in air [3, 29]. In those fibres with a low oxygen concentration, evolution of hydrogen gas is observed at $\sim 1300^\circ\text{C}$ [3]. This hydrogen possibly terminates the dangling bond in the fibre in a manner similar to the case of hydrogenated amorphous silicon. On the other hand, oxygen introduced through the curing process forms silicon oxide particles [29]. The carbon in the cured fibre reacts with the oxide at 1300°C [5].

The precipitation of carbon particles from the carbon-excess amorphous SiC may compete with the loss of carbon by the chemical reaction. The increase in the Raman intensity due to carbon indi-

cates that the precipitation rate is higher than the loss rate up to 1400°C . The loss rate overcomes the gain at $\sim 1500^\circ\text{C}$, and the amount of carbon particles decreases toward higher temperatures. Since the CO gas evolution at $\sim 1500^\circ\text{C}$ is observed in both cured and non-cured fibres [5], this gas evolution may be related to the reaction between carbon and oxygen contained in the starting material.

The CO gas evolution at $\sim 1500^\circ\text{C}$ correlates with the drastic increase in the SiC crystal size and to the decrease in the tensile strength down to virtually zero. Both phenomena occur for HTT between 1400 and 1500°C . The CO gas evolution at $\sim 1300^\circ\text{C}$, however, does not result in a big change in crystal size. The Raman data as mentioned in Section 3.1 suggest that the amount of carbon particle decreases above 1500°C . These experimental results indicate that the sudden increase in the crystal size occurs after a sufficient loss of carbon particles in number and/or size. Thus we find an important role of carbon particles, in that they separate SiC particles to suppress their growth and coalescence. Another role of the carbon particles may be to hold the SiC particles together. Carbon serves such a purpose because a single layer of the carbon microcrystal can fill gaps between SiC or silicon oxide particles on account of its flexible structure*. Oxygen contained in the fibres degrades their mechanical properties through chemical reaction with the carbon particles.

5. Conclusion

Analyses of the Raman spectra, X-ray diffraction and TEM photographs of the SiC fibre indicate that the fibre with the highest tensile strength consists of carbon and SiC microcrystals (~ 1 nm) distributed uniformly in carbon-rich amorphous SiC. The carbon particles play an important role for the high tensile strength of the SiC fibre i.e. they suppress growth and coalescence of the SiC microcrystals; furthermore, they may hold the SiC particles together. The growth of SiC crystals reduces the bonding forces at the grain boundaries. Oxygen introduced into the fibre in the curing process reduces the tensile strength at a high temperature, where carbon is lost through its chemical reaction with oxygen contained in the fibre.

References

1. "Strong Fibres and Composites", *Phil. Trans. R. Soc. A294* (1980) 407–597.
2. S. YAJIMA, *ibid.* A294 (1980) 419.
3. Y. HASEGAWA and K. OKAMURA, *J. Mater. Sci.* **18** (1983) 3633.
4. S. YAJIMA, K. OKAMURA, T. MATSUZAWA, Y. HASEGAWA and T. SHISHIDO, *Nature* **279** (1979) 706.
5. K. OKAMURA, M. SATO, T. MATSUZAWA and Y. HASEGAWA, *Polym. Prepr.* **25** (1984) 6.
6. S. HAYASHI, M. ITO and H. KANAMORI, *Solid State Commun.* **44** (1982) 75.
7. S. HAYASHI and H. ABE, *Jpn. J. Appl. Phys.* **23** (1984) L824.
8. S. HAYASHI, *Solid State Commun.* **56** (1985) 375.
9. L. L. ABELS, S. SUNDARAM, R. L. SCHMIDT and J. COMAS, *Appl. Surf. Sci.* **9** (1981) 2.

*The basal layer of graphite is reported to be much more flexible than that of clays, because the basal layer of clay consists of several atomic layers and has three-dimensional interatomic bonds [30].

10. Y. SASAKI, M. SATO, K. OKAMURA and Y. NISHINA, *Sci. Rep. Res. Inst. Tohoku Univ., Ser. A* **32** (1985) 111.
11. K. KUNC, M. BALKANSKI and A. NUSIMOVICI, *Phys. Status Solidi (b)* **72** (1975) 229.
12. M. H. BRODSKY and M. CARDONA, *J. Non-Cryst. Solids* **31** (1978) 81.
13. J. S. LANIN, L. J. PILONE, S. T. KSHIRSAGAR, R. MESSIER and R. C. ROSS, *Phys. Rev.* **B26** (1982) 3506.
14. A. R. VERMA and P. KRISHNA, "Polymorphism and Polytypism in Crystals" (Wiley, New York, 1966) Ch. 5 and 8.
15. D. OLEGO and M. CARDONA, *Phys. Rev.* **B25** (1982) 1151.
16. D. W. FELDMAN, J. H. PARKER Jr, W. J. CHOYKE and L. PATRICK, *ibid.* **173** (1968) 787.
17. *Idem*, *ibid.* **170** (1968) 698.
18. P. KRISHNA, R. C. MARSHALL and C. E. RYAN, *J. Cryst. Growth* **8** (1971) 129.
19. S. HAYASHI, *Jpn. J. Appl. Phys.* **23** (1984) 665.
20. L. GENZEL and T. P. MARTIN, *Phys. Status Solidi (b)* **51** (1972) 91.
21. R. TUINSTRA and J. L. KOENING, *J. Chem. Phys.* **53** (1970) 1126.
22. B. S. ELMAN, M. SHAYEGAN, M. S. DRESSELHAUS, H. MAZUREK and G. DRESSELHAUS, *Phys. Rev.* **B25** (1982) 4142.
23. R. B. LAUGHLIN and J. D. JOANNOPOULOS, *ibid.* **B16** (1977) 2942.
24. Y. IGUCHI, S. KASHIO, T. GOTO, Y. NISHINA and T. FUWA, *Can. Metall. Quart.* **20** (1981) 51.
25. N. WADA and S. A. SOLIN, *Physica* **105B** (1981) 353.
26. M. H. GRIMSDITCH and A. K. RAMDAS, *Phys. Rev.* **B11** (1975) 3139.
27. D. A. ANDERSON and W. E. SPEAR, *Phil. Mag.* **35** (1976) 1.
28. Y. INOUE, S. NAKASHIMA, A. MITSUISHI, S. TADA and S. TSUBOI, *Solid State Commun.* **48** (1983) 1071.
29. K. OKAMURA, M. SATO and Y. HASEGAWA, *J. Mater. Sci. Lett.* **2** (1983) 769.
30. B. R. YORK, S. A. SOLIN, N. WADA, R. H. RAYTHATHA, I. D. JOHNSON and T. J. PINNAVAIA, *Solid State Commun.* **54** (1985) 475.

*Received 3 March
and accepted 22 May 1986*